Results in Physics 12 (2019) 1294–1298

Contents lists available at ScienceDirect

Results in Physics

journal homepage: www.elsevier.com/locate/rinp

Electronic structure and optical response for $Zn_{1-x}Be_xSe$

Abdelaziz Gassoumi[a,b,*], Ali M. Alshehri[a], Nadir Bouarissa[c]

[a] King Khalid University, Faculty of Science, Department of Physics, P.O. Box 9004, Abha 61413, Saudi Arabia
[b] Université de Tunis El Manar, Faculté des Sciences de Tunis, Laboratoire de Physique de la Matière Condensée, 2092 Tunis, Tunisia
[c] Laboratory of Materials Physics and its Applications, University of M'sila, 28000, M'sila, Algeria

ARTICLE INFO

Keywords:
Band structure
Optical properties
$Zn_{1-x}Be_xSe$ alloys
FP-LAPW method

ABSTRACT

The electronic structures and optical properties of the $Zn_{1-x}Be_xSe$ semiconductor ternary alloys have been investigated by using the full-potential linear augmented plane wave (FP-LAPW) method. From this study, the energy band gap has a value of about 1.2 eV for zinc-blende ZnSe. However, for $Zn_{0.50}Be_{0.50}Se$ and BeSe, the fundamental band gap energy is found to occur at the highly symmetric X point in the Brillouin zone and has values of about 2.3 eV and 2.8 eV, for $Zn_{0.50}Be_{0.50}Se$ and BeSe, respectively. Optical parameters, such as dielectric constant, refractive index and reflectivity are calculated and analyzed. The results demonstrated that the compounds $Zn_{1-x}Be_xSe$ have the potential to be used for optoelectronic applications.

Introduction

Beryllium chalcogenides BeX (X = S, Se, Te) are interesting materials for optoelectronic devices operating in blue and ultraviolet spectral regions. This is due to their wide energy band gaps [1–4]. Beryllium selenide (BeSe) is an indirect band gap material with the highest valence band edge at the high-symmetry point Γ and lowest conduction band edge at X point [5–7]. It crystallizes in cubic zinc-blende structure. The interest in this binary semiconductor compound comes from the ternary BeZnSe and quaternary BeMgZnSe semiconductor compounds can be lattice matched to Si substrates [8] opening the approach to an Si-based optoelectronics devices. Moreover, the partial substitution of Zn by Be can improve the properties of the material of interest offering thus an impact in the improvement of ZnSe-based optoelectronics [1,3,9].

$Zn_{1-x}Be_xSe$ semiconductor ternary alloys are of potential interest for laser applications [1] and short wavelength optoelectronic applications [10]. These applications include engine control, flame sensors, plasma diagnostics and ozone monitors [10,11]. The properties of $Zn_{1-x}Be_xSe$ compounds have been investigated [5,9,10,12–14]. However, an accurate knowledge of the properties of $Zn_{1-x}Be_xSe$ are required in order to take advantage for any eventual technological applications. Furthermore, the present contribution reports on the calculations of the electronic structures and optical response of $Zn_{1-x}Be_xSe$ semiconductor ternary alloys using the full potential linearized augmented plane wave (FP-LAPW) method based on the density functional theory (DFT), within the mBJ-GGA approach.

Computational methodology

All the calculations in the present study, for $Zn_{1-x}Be_xSe$ compounds have been performed using the FP-LAPW method [15] using the DFT as implemented in the Wien2k package [16]. We have applied the mBJ-GGA approach for improving the accuracy of the electronic structures and their related optical properties. The convergence parameters R_{MT}*k_{max} is taken to be 8, the l_{max} equal to 10. The charge density is obtained up to G_{max} = 12 (a.u.)$^{-1}$. The convergence tolerance is chosen to be less than 0.10 mRy for the minimum energy.

Results and discussion

Fig. 1 illustrates the band structures of zinc blende ZnSe, $Zn_{0.50}Be_{0.50}Se$ and BeSe semiconducting materials along selected high-symmetry directions in the Brillouin zone computed using the mBJ-GGA approach. The Fermi energy level is taken to be as zero energy. Note that the overall features of these bands are qualitatively similar and differ only in details. From the quantitative point of view, they differ mainly in their fundamental band gap. The latter is found to occur at the highly symmetric Γ point in the Brillouin zone and has a value of about1.2 eV for zinc-blende ZnSe. However, for $Zn_{0.50}Be_{0.50}Se$ and BeSe, the fundamental band gap energy is found to occur at the highly symmetric X point in the Brillouin zone and has values of about2.3 and 2.8 eV, for $Zn_{0.50}Be_{0.50}Se$ and BeSe, respectively. The calculated fundamental energy band gap of ZnSe seems to be underestimated with respect to that of 2.721 eV from the experimental results

* Corresponding author.
E-mail addresses: agassoumi@kku.edu.sa, abdelaziz.gassoumi@gmail.com (A. Gassoumi).

https://doi.org/10.1016/j.rinp.2019.01.027
Received 9 December 2018; Received in revised form 6 January 2019; Accepted 8 January 2019
Available online 11 January 2019

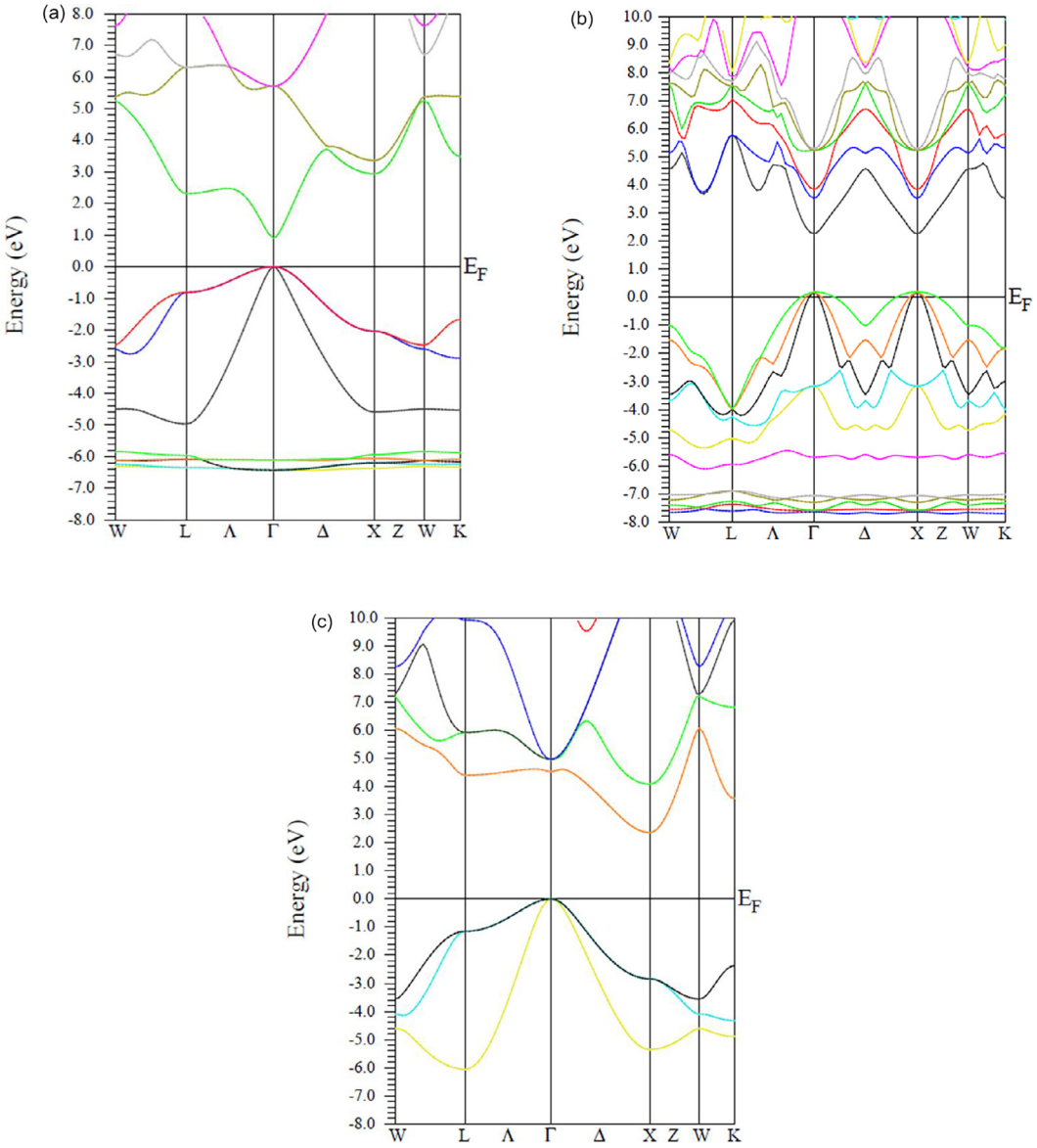

Fig. 1. Band structures (a) zinc-blende ZnSe (b) zinc-blende $Zn_{0.50}Be_{0.50}Se$ (c) Zinc-blende BeSe.

reported in Ref. [17]. The underestimation of the band gap is a well-known limitation of GGA calculation. There is no experimental data reported so far for the fundamental energy band gaps of $Zn_{0.50}Be_{0.50}Se$ and BeSe, to the best of our knowledge. Nevertheless, Grein et al. [10] reported a theoretical value of 2.65 eV obtained from the generalized DFT calculations for the indirect band gap at X point for BeSe. This value is in reasonable accord with that calculated in the present work. It is to be noted that even our value is underestimated with respect to that of experiment, it gives better accord with respect to experiment than previous GGA calculations. The better accord between our results and those from experiment and previous calculations is not surprising since mBJ-GGA approach has been proved to give more accurate values than other GGA approaches regarding the energy band gaps [18–20]. The behavior of the valence bands is that expected from the combinations of the bonding of hybridized atomic sp^3 orbitals. The maxima of the valence bands are flat suggesting thus large hole effective masses, that result in some specific transport properties for semiconductors of type p. The valence bands appear to be less dispersive than the conduction bands. This is due to the fact that the valence bands are less delocalized than the conduction bands.

The partial and total density of states (DOS) of the zinc-blende BeSe and $Zn_{1-x}Be_xSe$ (x = 0.50) semiconductor materials are plotted in Fig. 2. Note that the Se p states in the valence bands of BeSe are dominant below 0 eV, whereas in the conduction bands, the Se d states and Be p states are the most dominant. As regards $Zn_{0.50}Be_{0.50}Se$ semiconductor ternary alloy, the Se p states in the valence bands have the dominant contribution below 0 eV, whereas in the conduction bands, the Se p and Zn s are the most dominant in the energy range lying between 2 and 4.5 eV and the Se p and Zn p are the most dominant in the energy range lying between 4.5 up to 8 eV. The peaks that correspond to Se 4s, Be 2s, Zn 3d and Se 4p are clearly shown in Fig. 2. These peaks present four essential regions. The first region is predominantly Se 4s states. The rest of the regions are made of Be 2s, Zn 3d and Se 4p. As one goes from BeSe to $Zn_{1-x}Be_xSe$ (x = 0.50) the peaks are shifted either up or down in energy. This is traced back to the variation in nearest-neighbor bond lengths as well as in the change in the total symmetry.

The knowledge of the optical properties of semiconductor materials are very important for numerous applications such as photo-detectors, lasers and light emitting diodes. The optical properties are highly related to the electronic band structure of the semiconductor material and can be obtained readily from it. In the present contribution the real

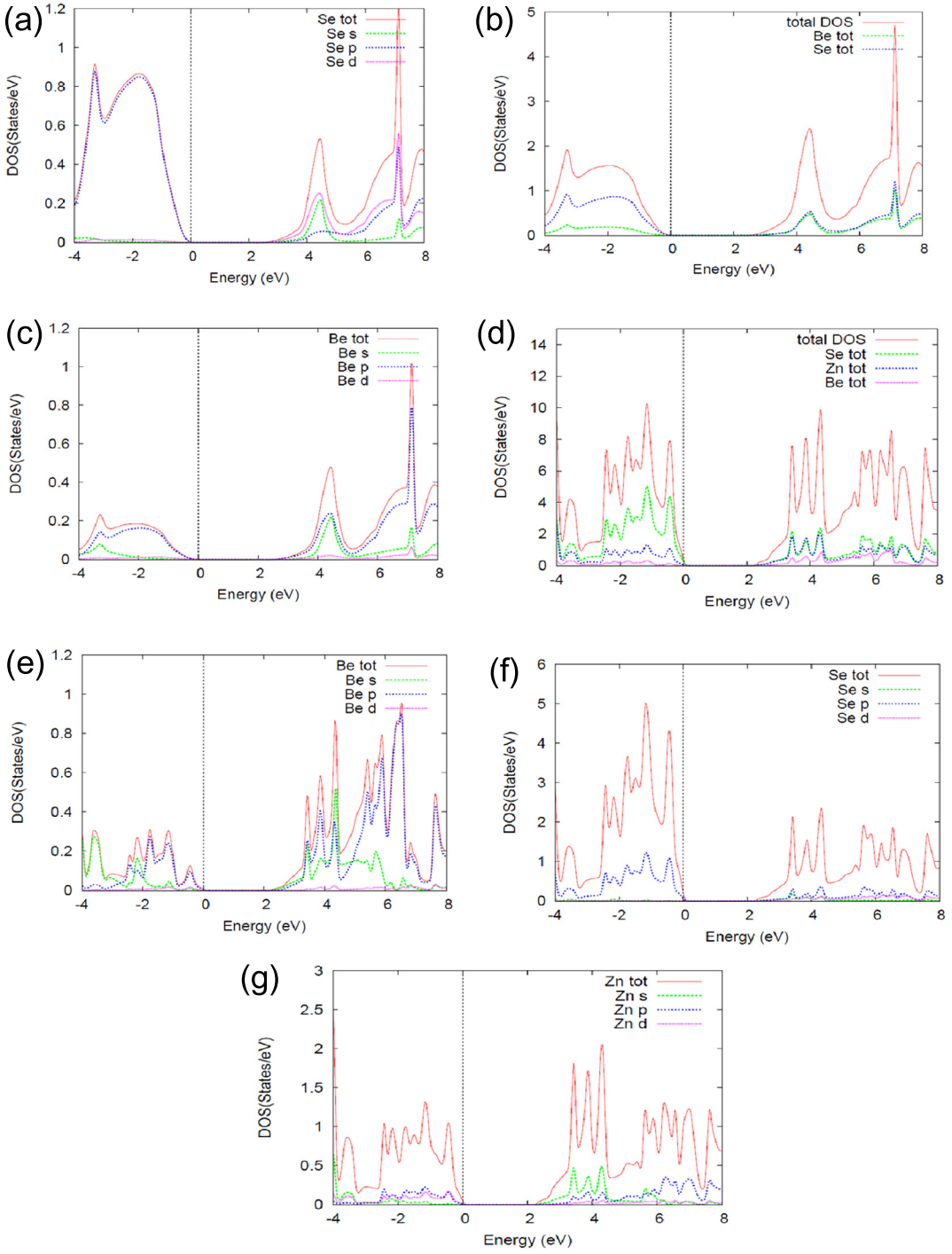

Fig. 2. Partial and total density of states (DOS) of (a, b, c) zinc-blende BeSe and (d, e, f, g) zinc-blende $Zn_{0.50}Be_{0.50}Se$.

$\varepsilon_1(E)$ and imaginary $\varepsilon_2(E)$ parts of the dielectric function have been computed for $Zn_{1-x}Be_xSe$ at various concentrations, where E is the photon energy, using the following equations,

$$\varepsilon_2(\omega) = \frac{e^2\hbar}{\pi\, m^2\omega^2} \sum_{V,C} \int_{BZ} |M_{CV}(k)|^2 \delta\,[\omega_{CV}(k) - \omega] d^3k \tag{1}$$

$M_{CV}(k)$ in Eq. (1) represent the transition moments elements, whereas $\hbar\omega_{CV}(k) = E_{Ck} - E_{Vk}$ is the excitation energy.

$$\varepsilon_1(\omega) = 1 + \frac{2}{\pi} P \int_0^{\infty} \frac{\omega'\varepsilon_2(\omega')}{\omega'^2 - \omega^2} d\omega' \tag{2}$$

where P implies the principal value of the integral.

Our results are shown in Figs. 3 and 4, for $\varepsilon_1(E)$ and $\varepsilon_2(E)$, respectively. Note that both $\varepsilon_1(E)$ and $\varepsilon_2(E)$ behave almost in the similar manner when varying the alloy concentration x on going from 0 (ZnSe) to 1 (BeSe). This is generally common for the III-V and II-VI tetrahedral bonded semiconductors [21–23]. Usually, the main difference lies in their transition energies. The principal peak of the real part for ZnSe (x = 0) occurs at approximately E ≈ 6 eV, whereas that of BeSe (x = 1) occurs at around E ≈ 2.9 eV (see Fig. 3). The peak shifts towards different energies when the alloy content x is changed. This can be attributed to the inter-band transitions. The shape of $\varepsilon_1(E)$is generally that expected for a harmonic oscillator which has a resonant frequency of around 6.25 eV in our case for ZnSe (x = 0) and at approximately

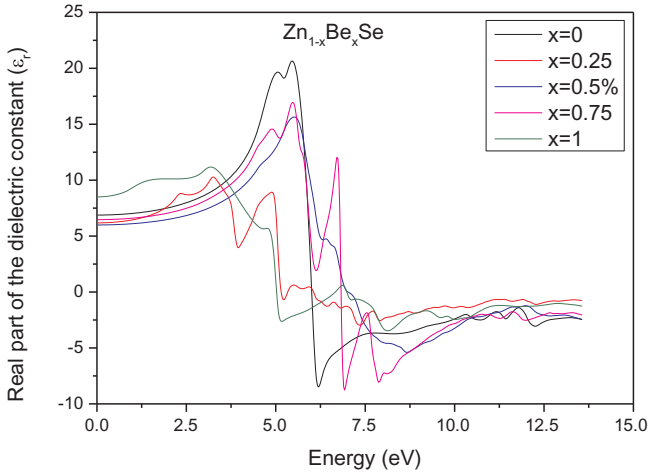

Fig. 3. Real part of the dielectric function for $Zn_{1-x}Be_xSe$ at various Be concentrations x.

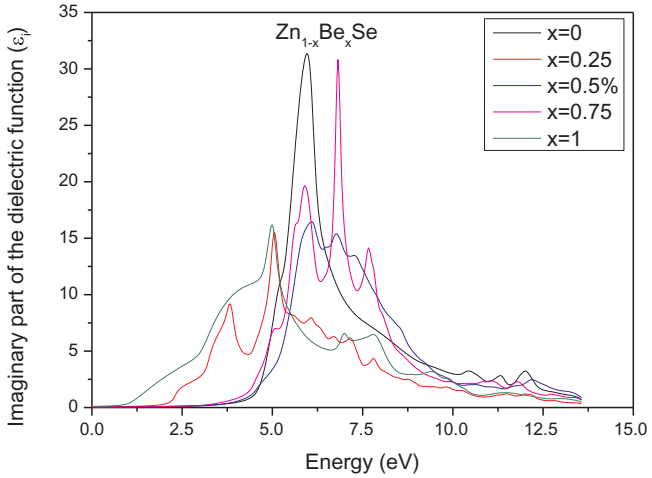

Fig. 4. Imaginary part of the dielectric function for $Zn_{1-x}Be_xSe$ at various Be concentrations x.

7.9 eV for BeSe (x = 1). When varying the alloy composition x, the resonant frequency shifts towards higher or lower energies depending on x.

Focusing on $\varepsilon_2(E)$, there are three main peaks in the $\varepsilon_2(E)$plot of the zinc-blende $Zn_{1-x}Be_xSe$ phase. The $\varepsilon_2$curve is zero below the onset of direct interband transitions. It starts with the E_0-type transition at Γ, which corresponds to the fundamental energy band gap. Then, it increases steeply for a photon energy larger than the value of the fundamental energy band gap to reach $\varepsilon_2 \approx 4$ at about 5 eV in the case of ZnSe. The steep increase in $\varepsilon_2$above the photon energy of the fundamental band gap can be traced back to the onset of direct interband transitions at the high symmetry Γ point in the Brillouin zone with a predicted gap of 1.2eVin the case of ZnSe. $\varepsilon_2$continues to rise to a maximum of $\varepsilon_2 \approx 32$ at around 6 eV. The peak in ε_2 is ascribed to a high joint DOS associated with nearly parallel bands near the high symmetry Γ point in the Brillouin zone. This peak is due to transitions from the highest valence bands to the lowest conduction band. After, ε_2 decreases rapidly to a minimum of ε_2. These arise mainly from regions at the Γ point. Note that by adding Be into ZnSe results in the shift of all main peaks. It changes the peaks intensity suggesting the change of the absorption which starts for the ε_2 at about 1.2 eV in the case of ZnSe. The variation of the alloy composition x does not seem to affect much the overall shape of $\varepsilon_2(E)$. The main difference between $\varepsilon_2(E)$at various alloy concentrations x lies in the transition energies.

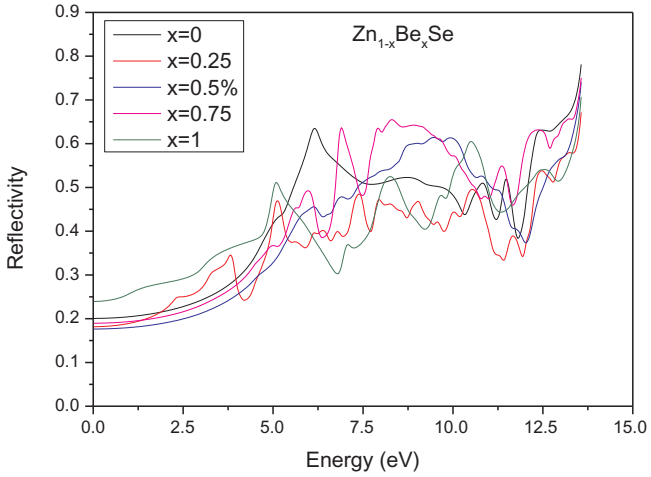

Fig. 5. Reflectivity spectrum for $Zn_{1-x}Be_xSe$ at various Be concentrations x.

The reflectivity spectrum of $Zn_{1-x}Be_xSe$ at different concentrations is shown in Fig. 5. It is derived from the complex dielectric function. Note that the reflectivity spectrum of the zinc-blende $Zn_{1-x}Be_xSe$ phase at various concentrations x shows some peaks at around 5, 6 and 7 eV depending on the alloy concentration x. These peaks reflect the interband transitions from the valence to conduction bands. The peak of the reflectivity is reduced as the composition x is increased with a shift of peaks towards high or low energies depending on x. The peaks are affected in both the sharp and broadening. This is consistent with the results of Gueddim et al. [24] reported for $ZnTe_{1-x}O_x$ semiconductor ternary alloys.

The absorption coefficient gives information about the penetration of light of a particular wavelength into the material under study before it is absorbed. The variation of this parameter versus the photon energy is illustrated in Fig. 6. Note that the peaks of the absorption coefficient spectra vary in magnitude when proceeding from x = 0 (ZnSe) to x = 1 (BeSe). The magnitude of these peaks depends on the alloy composition x. It depends also on the energy of light being absorbed. The absorption coefficient for x = 0 at around a photon energy of 6 eV is higher than that for x = 1. Thus, the absorption of light in BeSe is poor as compared to that in ZnSe at that photon energy. On the other hand, we observe that the absorption at low photon energies is relatively low. This is due to the fact that only the electrons located at the valence band edge can contribute to the absorption. By increasing the photon energy, the value of the absorption coefficient becomes higher. This can be traced back to

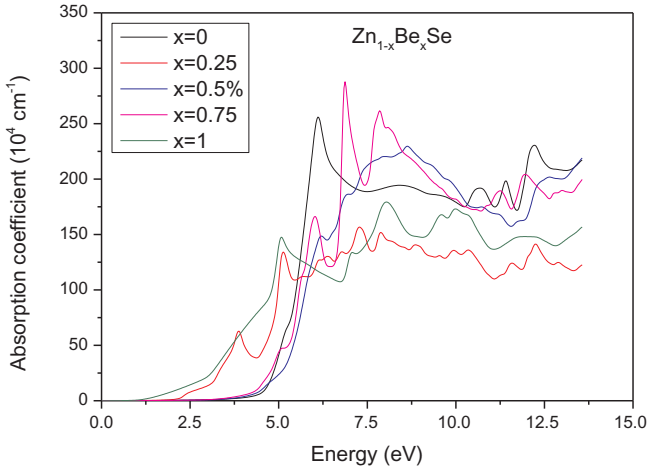

Fig. 6. Optical absorption coefficient spectrum for $Zn_{1-x}Be_xSe$ at various Be concentrations x.

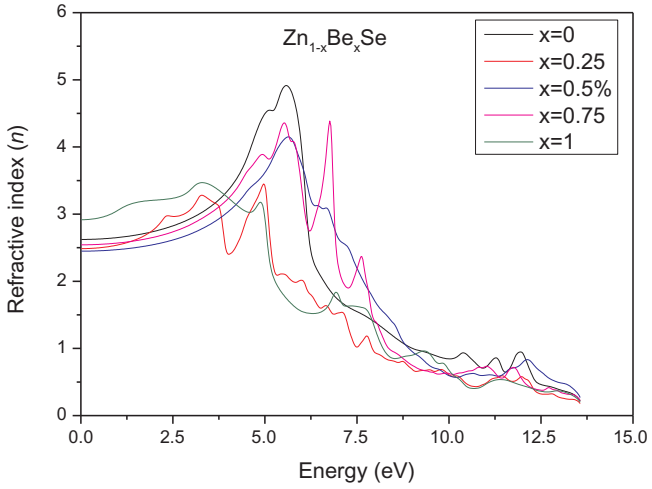

Fig. 7. Refractive index spectrum for $Zn_{1-x}Be_xSe$ at various Be concentrations x.

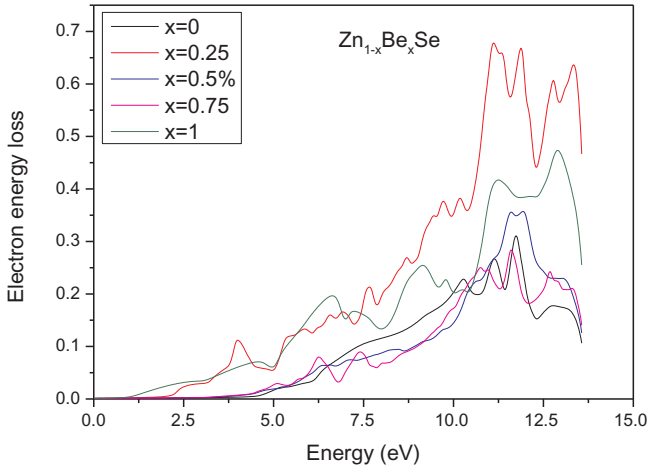

Fig. 8. Electron energy loss spectrum for $Zn_{1-x}Be_xSe$ at various Be concentrations x.

the increase of the number of electrons, which interact with the photon increasing thus the number of absorbed photons.

The refractive index spectrum as a function of photon energy for $Zn_{1-x}Be_xSe$ at different Be concentrations ranging from x = 0 (ZnSe) to x = 1 (BeSe) is computed using mBJ-GGA approach. Our results are displayed in Fig. 7. We observe clear peaks which are originated from the excitonic transitions at the E_0 edges. As one proceeds from x = 0 (ZnSe) to x = 1 (BeSe), these peaks shift towards lower or higher energies. The shift depends strongly on the alloys content x. The most important peak in the refractive index spectra is essentially related to the 2 D exciton. transition (E_1). Its position depends also strongly on the alloy concentration x. It has been reported in the literature that the excitonic effects have tendency to increase the oscillator strength at the critical points M_0 and M_1 [25]. This gain must be compensated by losses elsewhere. For ZnSe (x = 0), the static refractive index is found to be about 2.57, whereas for BeSe (x = 1), its value has been determined to be around 2.9. Our obtained static refractive index for ZnSe agrees well with that of 2.51 calculated by Hannachi and Bouarissa [26] using the empirical pseudopotential method and that of 2.5 quoted in Ref. [27]. As far as our static refractive index for BeSe is concerned, our result is only for reference.

In order to describe the energy loss of fast electrons penetrating the material of interest, results of the electron-energy-loss function for $Zn_{1-x}Be_xSe$ at various concentrations are plotted in Fig. 8. In the spectra shown in Fig. 8, the peaks are the characteristic associated with the plasma resonance in which the corresponding frequency is usually called plasma frequency. These peaks correspond to the trailing edges in the reflection spectra. We observe small peaks at lower energies followed by a broad plasma resonance at approximately 11.5 eV. Similar qualitative behavior has been reported for the electron-energy loss function of ZnS using ab initio molecular dynamics simulation at different temperatures [28]. By varying the alloy content x, we note a slight shift of the plasma frequencies towards lower energies with a small change in the spectrum shape.

Conclusion

We have investigated the electronic structures and optical properties of the $Zn_{1-x}Be_xSe$ ternary semiconductor alloysin the zinc-blende phase using the FP-LAPW method. Band gap dependent optical constants like the dielectric function, the refractive and reflectivity were investigated based on the mBJ-GGA approach. We calculated the real $\varepsilon_1(\omega)$ and the imaginary $\varepsilon_2(\omega)$ parts of dielectric function. For ZnSe (x = 0), the static refractive index is found to be about 2.57, whereas for BeSe (x = 1), its value has been determined to be around 2.9. We have also calculated the refractive index $n(\omega)$, the extinction coefficient $k(\omega)$, the energy-loss $L(\omega)$ and the reflectivity $R(\omega)$. The electronic structure and optical results in our investigation demonstrate promising applications of $Zn_{1-x}Be_xSe$ compounds for optoelectronic device technologies.

Acknowledgement

The authors are thankful to the Deanship of Scientific Research to Research Center of Advanced Materials at King Khalid University in Saudi Arabia for support this research.

References

[1] Waag A, Fischer F, Schüll K, Baron T, Lugauer H-J, Litz Th, et al. Appl. Phys. Lett. 1997;70:280.
[2] Zhang JY, Shen DZ, Fan XW, Yang BJ, Zheng ZH. J. Cryst. Growth 2000;214–215:100.
[3] F. Firszt, S. ŁĮgowski, H. Męczyriska, J. Szatkowski, W. Paszkowicz, K. Godwod, J. Cryst. Growth 184/185 (1998) 1335.
[4] Saib S, Bouarissa N. Solid State Sci 2010;12:563.
[5] Adachi S. Properties of Semiconductor Alloys: Group-IV, III-V, and II-VI Semiconductors. Chichester: Wiley; 2009.
[6] Stukel DJ. Phys. Rev. B 1970;2:1852.
[7] Muñoz A, Rodríguez-Hernández P, Mujica A. Phys. Stat. Sol. (b) 1996;198:439.
[8] Chauvet C, Bousquet V, Tournié E, Faurie JP. J. Electron Mater 1999;28:662.
[9] Wronkowska AA, Bukaluk A, Wronkowski A, Trzciński M, Firszt F, Legowski S, et al. Surf. Sci. 2002;507–510:170.
[10] Grein CH, Radtke RJ, Ehrenreich H, Chauvet C, Tournié E, Faurie JP. Solid State Commun. 2002;123:209.
[11] Faurie JP, Bousquet V, Brunet P, Tournié E. J. Cryst. Growth 1998;184(185):11.
[12] Hwang Y, Kim H, Um Y, Furdyna JK. J. Korean Phys. Soc. 2007;50:858.
[13] Bhalerao GM, Polian A, Gauthier M, Itié J-P, Baudelet F, Ganguli T, et al. J. Appl. Phys. 2010;108:083533.
[14] Pagès O, Ajjoun M, Bormann D, Chauvet C, Tournié E, Faurie JP. Phys. Rev. B 2002;65:035213.
[15] Gassoumi A, M. Musa Saad H-E. Mat. Sci. Semicon. Proc. 2016;50:14.
[16] Blaha P, Schwarz K, Medsen GKH, Kvasnicka D, Luitz J. Karlheinz Schwartz. Wien, Austria: Techn. Universitad; 2001.
[17] Adachi S. Properties of Group-IV, III-V, and II-VI Semiconductors. Chichester: Wiley; 2005.
[18] A. Gassoumi,A. Al-Shahrani, S. Alfaify, H. Algarni, R. Vidu, J. Optoelectron. Adv. M. 20 (9-10) (2018) 453.
[19] Gassoumi A, Meradji H, Kamoun-Turki N, Ghemid S. Mat. Sci. Semicon. Proc. 2015;40:262.
[20] Gassoumi A, M. Musa Saad H-E, Alfaify S, Ben Nasr T, Bouarissa N. J. Alloy. Compd. 2017;725:181.
[21] Cohen ML, Chelikowsky JR. Electronic Structure and Optical Properties of Semiconductors. Berlin: Springer-Verlag; 1988.
[22] Bouarissa N, Gueddim A, Siddiqui SA, Boucenna M, Al-Hajry A. Superlatt. Microstr. 2014;72:319.
[23] Bellouche A, Gueddim A, Zerroug S, Bouarissa N. Optik 2016;127:11374.
[24] Gueddim A, Zerroug S, Bouarissa N. J. Luminescence 2013;135:243.
[25] Yu PY, Cardona M. Fundamentals of Semiconductors, Physics and Materials Properties. Berlin-Heidelberg: Springer-Verlag; 1996.
[26] Hannachi L, Bouarissa N. Phys. B 2009;404:3650.
[27] D. W. Palmer, < www.semiconductors.co.uk > , 2008.03.
[28] Khan MA, Bouarissa N. Optik 2013;124:5095.